Int. J. Electrochem. Sci., 11 **(2016)** 9402 – 9412, doi: 10.20964/2016.11.54

International Journal of ELECTROCHEMICAL SCIENCE
www.electrochemsci.org

Electrocatalytic Oxidation of Formic Acid in Acid Medium at Pd Electrodeposited onto TiO_2 Nanotubes

J. Aldana-González[1, 2], *J. Uruchurtu-Chavarin*[2], *M. G. Montes de Oca*[1], *M. T. Ramírez-Silva*[3], *M. Palomar-Pardavé*[1], *M. Romero-Romo*[1,*]

[1] Universidad Autónoma Metropolitana Azcapotzalco. Departamento de Materiales, Av. San Pablo #180, Col. Reynosa-Tamaulipas, CDMX, C.P. 02200, Mexico
[2] Universidad Autónoma del Estado de Morelos. CIICAP. Av. Universidad No. 1001, Col. Chamilpa, Cuernavaca. C.P. 62209, Morelos, México.
[3] Universidad Autónoma Metropolitana-Iztapalapa, Departamento de Química, Av. San Rafael Atlixco #186, Col. Vicentina, CDMX, C.P. 09340, Mexico
[*]E-mail: mmrr@correo.azc.uam.mx

Received: 6 July 2016 / *Accepted:* 9 September 2016 / *Published:* 10 October 2016

TiO_2 nanotubes were electrolytically formed on a Ti surface after which Pd was electrodeposited for different times. The electrodes thus produced were evaluated for the HCOOH electro-oxidation in an acid aqueous solution. It is shown that the HCOOH oxidation current density varies as a function of the Pd electrodeposition time. The best performing electrode was that achieved after 1200 seconds Pd electrodeposition.

Keywords: Palladium; TiO_2 nanotubes; formic acid; oxidation.

1. INTRODUCTION

Consumption of fossil fuels increased significantly during the last century up until today, particularly to meet a growing energy demand associated to increases in population and industry activities. It is common knowledge that this has resulted in significant damage to the environment, largely caused by greenhouse gases that cause global warming, since they are the product of incomplete combustion of diverse fuels. The continued search for viable alternatives to meet the energy demands of the world is an ever growing social concern, which in the short term should aim at providing clean, sustainable, energy sources capable of rendering the means to minimize the rate of environmental impacts [1]. An excellent alternative is the use of fuel cells, that convert chemical energy directly into electricity with minimal or no pollution at all. Such devices have already an

important technological historic expanse [2, 3], although currently ongoing research is still looking for newer, better building materials to improve their performance while lowering costs. Direct formic acid fuel cells (DFAFCs) represent a good alternative for power generation, because they display efficiencies comparable to their counterparts using direct alcohol [4], although theoretically, they have higher electromotive cell force as compared with methanol and hydrogen [5], require less storage, transport and handling cares, compared to hydrogen-based cells [6, 7]. The most commonly used catalyst in fuel cells is Pt [8-11], although it displays outstanding disadvantages like low costly availability and surface poisoning of their active sites due to adsorption of reaction intermediates, such as CO [12]. In contrast to basic Pt catalysts, Pd has exhibited consistent results during catalytic electrooxidation of formic acid through a direct path that does not generate CO, which widens the overall capability and ensures longer utility of this metal catalysts [13-16]. Another important aspect is the influence of the catalysts supports, which generally are carbon-based materials [17-19], that increase the overall surface area. However, even when the catalyst action is strongly influenced by the carbonaceous support, another problem is carbon oxidation through oxidation processes of the organic molecules involved, so that the durability and time life of the cells based on such media decrease [20, 21]. Since the discovery of carbon nanotubes [22], there has been a growing interest in tubular-type nanostructured materials, mainly due to their outstanding electrical, mechanical and textural properties, namely porosity and large surface area, which make them excellent candidates for supporting catalysts [23]. TiO_2-based materials have, low toxicity, high thermal and mechanical stability, which make them attractive enough to be incorporated into various sorts of catalysts [24-26]. Therefore, this study proposes the use and application of third generation TiO_2 nanotubes, TiO_2-NTBs, as support for metallic Pd clusters, potentiostatically electrodeposited, without any additional treatment, thereby conforming an attractive, inexpensive technical proposition.

2. EXPERIMENTAL

2.1 Formation of TiO_2-NTBs by Ti anodizing

Cylinders 2.0 cm long were cut from a Ti (8.0 mm OD, purity 99.6+ %, Advent Research Materials LTD) rod, and then immersed in polyester resin, leaving only 0.502 cm^2 exposed area; the samples thus mounted were polished down to a surface mirror finish with alumina powder. After, they were cleansed in an ultrasonic bath with deionized water, acetone and dehydrated ethanol for 10 minutes per solution. The TiO_2 nanotube films were prepared by potentiostatic anodizing in a two-electrode cell using Pt as the cathode, and the Ti specimen as anode, in glycerol-water (50:50) and 0.5 wt% NH_4F medium, all solutions were prepared with deionized water (Ultra-pure water Type 1 from a Milli-Q Ultrapure Water System, 18.2 MΩ.cm @ 25 °C, TOC <10 ppb) and commercial analytical grade reagents. Ti anodizing was performed under constant stirring throughout the process, imposing 20 V constant potential by means of a DC power supply (BK Precision 1770) for 2 hours.

2.2 Pd Electrodeposition onto TiO_2-NTBs

Pd electrodeposition on TiO_2-NTBs (TiO_2-NTBs/Pd) was carried out through chronoamperometry, imposing a constant potential via the AUTOLAB PGSTAT 100 potentiostat-galvanostat, and a conventional three electrode electrochemical arrangement using TiO_2-NTBs as working electrode, a Pt wire as counter electrode, and a Ag / AgCl 3.0 M KCl as reference, to which all potentials stated in this work should be referred to. The supporting electrolyte was a 0.5 M H_2SO_4 and 3.0 mM $PdCl_2$ solution. The potential imposed on the electrode was −1.6 V for 0.1 s, as nucleation pulse, followed by a nuclei growth pulse of −0.2 V, for periods of 600, 1200, 1800, 2700 and 3600 s.

2.3 SEM characterization

SEM images were obtained through a JEM-1200EX SUPRA 55PV instrument from JEOL-Carl-Zeiss, equipped with energy dispersive spectroscopy (EDS).

2.4 Evaluation of the active surface area

The active surface area of TiO_2-NTBs/Pd electrode was evaluated by immersion in 0.5 M H_2SO_4, through which CO was bubbled for 15 min; thereafter N_2 was bubbled for 20 min. During these processes, the working electrode potential was kept at −0.17 V. Subsequently, CO oxidation was carried out potentiodynamically, within the −0.17 to 1.0 V potential window at 20 mVs^{-1}.

3. RESULTS AND DISCUSSION

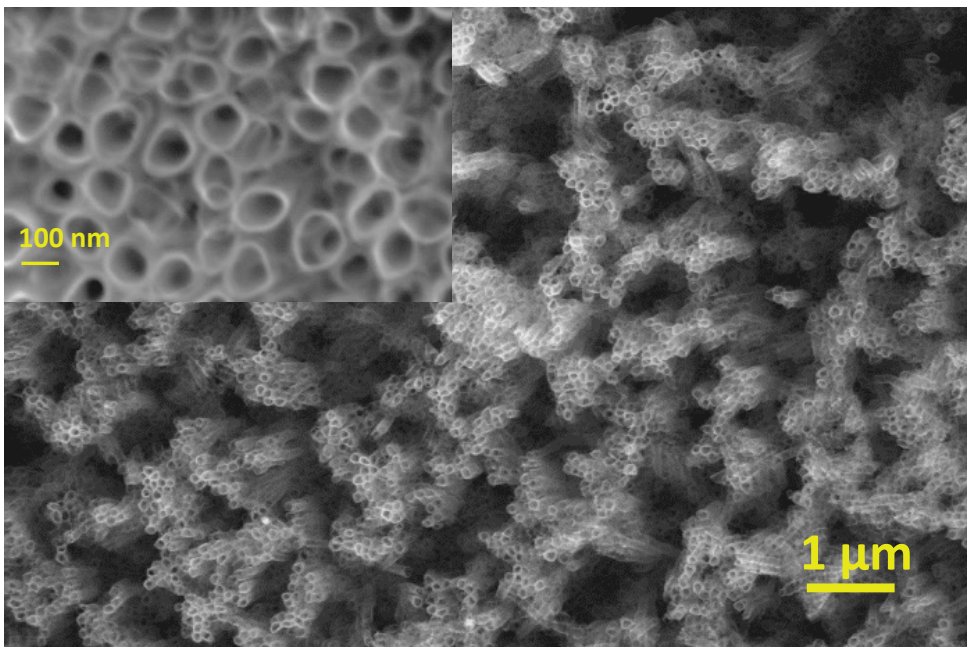

Figure 1. SEM image of TiO_2-NTBs formed after Ti anodization imposing 20 V constant potential for 2 hrs in glycerol-water (50:50) and 0.5% W NH_4F medium.

Figure 1 depicts the resulting morphology of the TiO_2-NTBs formed. Clusterings of single wall nanotubes, with an average diameter of (100 ± 5) nm can be observed. Overall, there appears that there was a relatively dense growth of TiO_2-NTBs that covered the whole electrode surface.

3.1 Cyclic voltammetry electrochemical characterization

One way to determine if the electrode undergoes a modification in its active surface is through cyclic voltammetry, based on the current response obtained. In this case, the study was performed comparing the TiO_2-NTBs electrode response with that of the bare Ti electrode. From Figure 2, it is possible to note an increase in the capacitive response of the electrode containing the TiO_2-NTBs and also the magnitude of the hydrogen evolution current, which begins to be noted right from 300 mV. This behavior is due to the presence of TiO_2-NTBs on the surface. This same behaviour has been reported by Yu et al. [27], by means of cyclic voltammetry studies of TiO_2 nanotube arrays electrode in the presence of H^+.

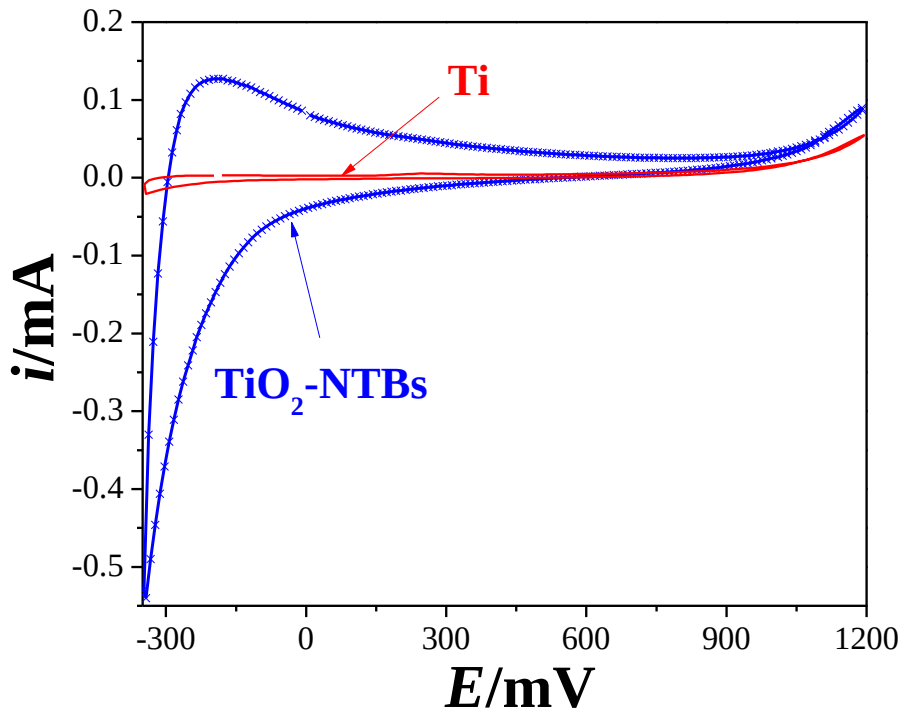

Figure 2. Comparison of CVs recorded using a bare Ti or TiO_2-NTBs immersed in 0.5 M H_2SO_4. The potential scan started at the respective open circuit potential value at 50 mVs^{-1} in the cathodic direction.

3.2 Pd electrodeposition onto the TiO_2-NTBs

Once formed and characterized the TiO_2-NTBs, the Pd electrodeposition process was done through chronoamperometry, CA. Figure 3 shows the SEM images of the TiO_2-NTBs surface modified

with electrodeposited Pd for different times. For 600 s, see Figure 3a, the Pd nuclei decorating the TiO_2-NTBs, are clearly seen, however for a longer time, Figure 3b, the Pd deposit depicts a dendritic morphology, such that it covered the whole surface of the TiO_2-NTBs. In both cases, the EDS analysis shows the presence of Pd and Ti.

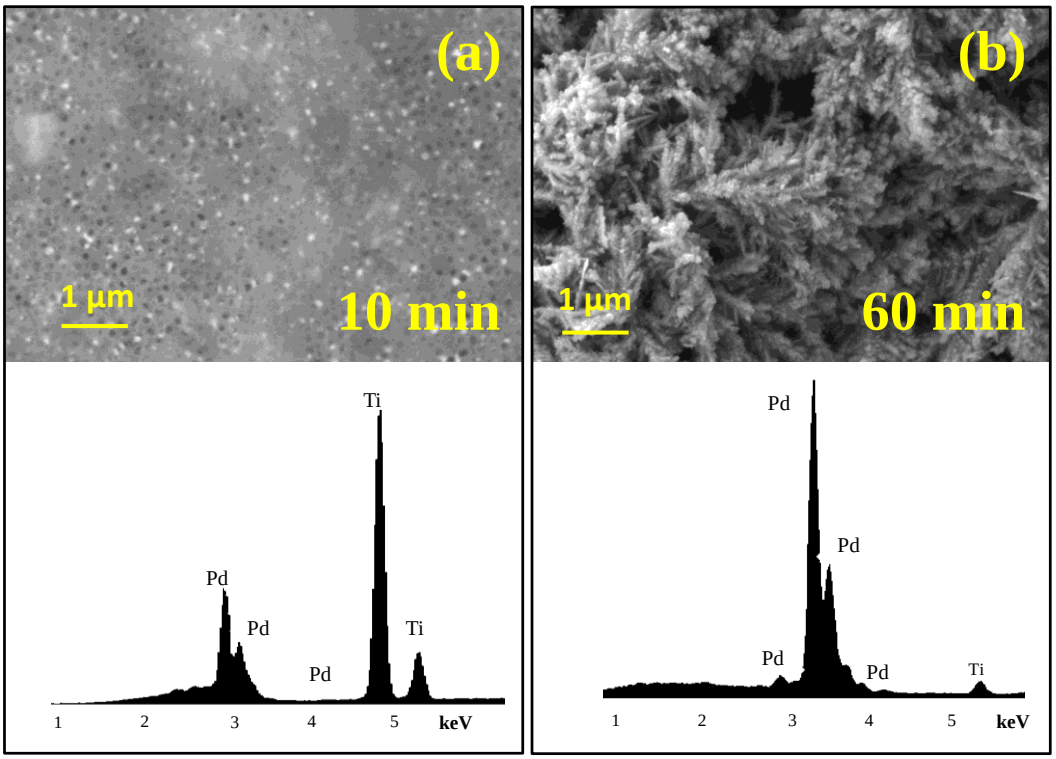

Figure 3. SEM images of Pd electrodeposited onto the TiO_2-NTBs surface after a) 600 and b) 3600 s. and its respective EDS analyses.

Figure 4a compares the corresponding CVs of the bare and Pd-modified TiO_2-NTBs electrodes. It can be seen, in the response of the Pd-modified electrode, that Pd oxidation started at *ca.* 600 mV, subsequently reaching a maximum at 1200 mV. Thereafter, during the reverse potential scan, Pd reduction begins at about 600 mV forming a well-defined peak. The notorious increase in the cathodic current that starts at around 0 mV, corresponds to proton reduction. Finally, after reversing the potential scan at approximately −375 mV, another oxidation peak is formed, displaying a current maximum at 100 mV, which is associated to the hydrogen oxidation process. In comparison, the hydrogen reactions onto the bare TiO_2-NTBs electrode are negligible. It results plain that the Pd-modified electrode has undergone a relevant modification due to the Pd presence on the surface of the TiO_2-NTBs, thereby promoting the hydrogen reactions. Figure 4b shows a comparison of three different electrodes, which underwent also potentiostatic Pd deposition for different times. An increase in both anodic and cathodic currents can be seen, which were favoured when the Pd electroplating time was increased.

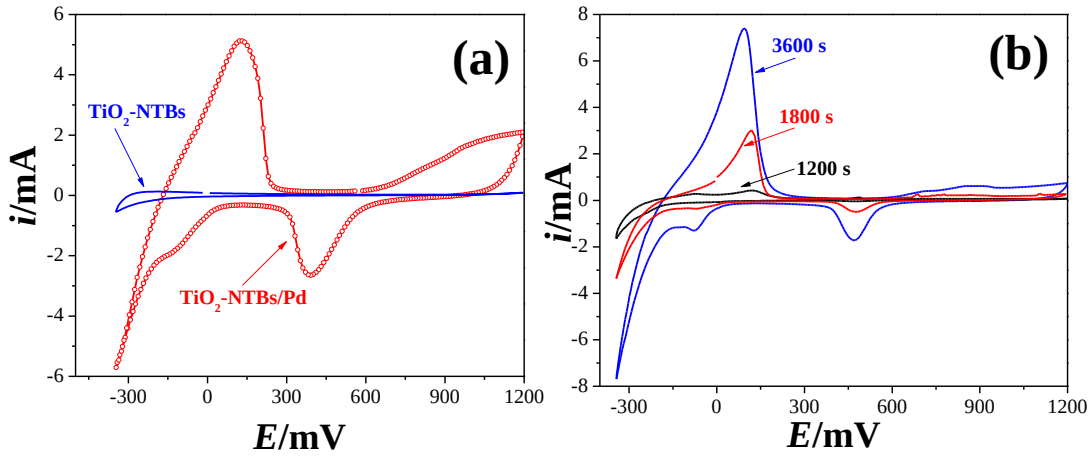

Figure 4. Comparison of CVs of a) TiO_2-NTBs or TiO_2-NTBs/Pd (deposited during 2700 s at −0.2 V) and b) TiO_2-NTBs/Pd for different times of Pd electrodeposition. In all cases, the electrodes were immersed in 0.5 M H_2SO_4 and the potential scan started at the respective open circuit potential value at 50 mV s^{-1} in the cathodic direction.

Figure 5 shows the CVs recorded with Pd electrodeposited on TiO_2-NTBs and Pd electrodeposited on the bare Ti. From the comparison of the CVs it becomes plain that when the Pd was electrodeposited on Ti metal, its electrochemical response fails to be significant in terms of hydrogen reactions, than when the metal had been deposited onto the TiO_2-NTBs. Moreover, even when Pd oxide formation and reduction occurs on Ti, see the inset in Figure 5, it is negligible in comparison with that of TiO_2-NTBs.

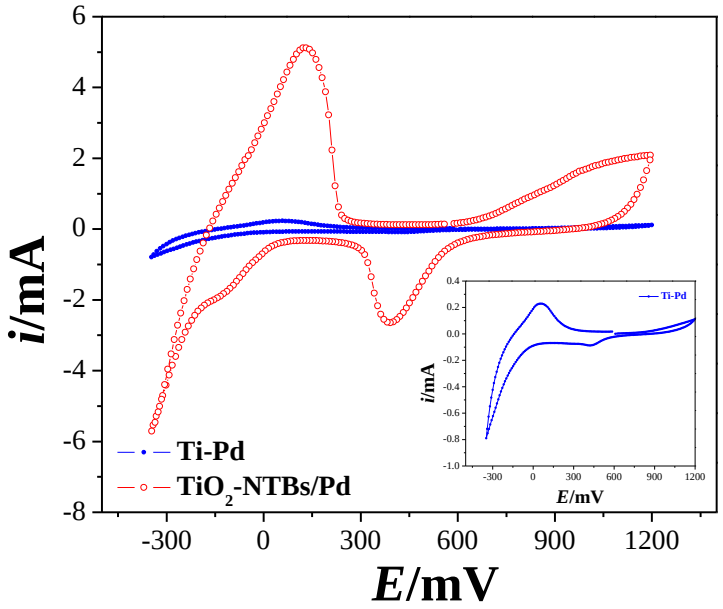

Figure 5. Comparison of CVs recorded using the TiO_2-NTBs/Pd or Ti/Pd electrodes (deposited during 2700 s at −0.2 V) immersed in 0.5 M H_2SO_4. In both cases, the potential scan started at the respective open circuit potential value at 50 mV s^{-1} in the cathodic direction. The inset shows a close up of the Ti/Pd electrode CV.

From Figure 5, the TiO_2-NTBs/Pd exhibit significant changes in the current density at potentials more negative than −0.2 V, with a strong cathodic peak close to −0.3 V and an anodic peak at −0.12 V: the processes occurring are hydrogen loading and desorption. The current originating from H evolution becomes predominant at potentials more negative than −0.27 V. It is important to mention that Wang et al., [28] have studied the activity of novel Pd/TiO2 nanotube catalysts for methanol electro-oxidation reported a very similar CV as that depicted in Figure 4 and 5.

3.3 Active surface area evaluation

Figure 6 shows the CVs recorded during the CO oxidation on TiO_2-NTBs/Pd (cycle 1). The cycle 2 was recorded after CO removal depicting the typical Pd electrochemical behaviour in acid media [29, 30]. From the ratio between the oxidation charge recorded during cycle 1 and that corresponding to the formation of the CO monolayer onto polycrystalline Pd [31], the active surface area was obtained; the longer the deposition time the greater the active surface area. From these areas the corresponding current density, *j*, was obtained.

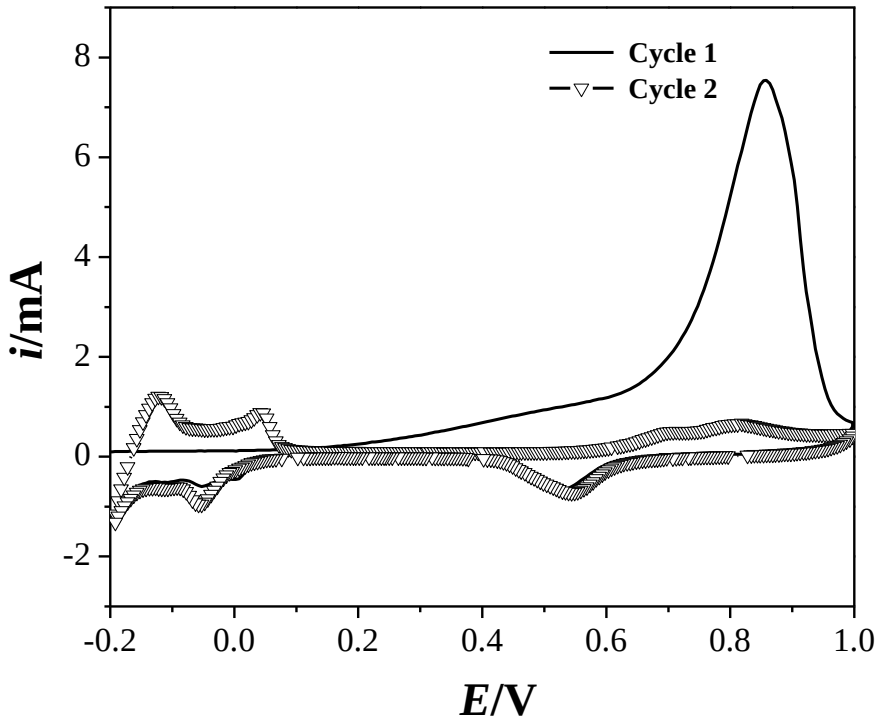

Figure 6. CVs recorded during CO desorption from TiO_2-NTBs/Pd.

3.4 Formic acid oxidation using the TiO_2-NTBs/Pd electrode

Figure 7 shows linear voltammograms recorded during the HCOOH oxidation using different TiO_2-NTBs/Pd electrodes. It is possible to note that both the current density and potential peak of

HCOOH oxidation varied, depending on the Pd electrodeposition time onto the TiO_2-NTBs electrodes. From 600 to 1800 s the peak potential moved toward more positive values while the respective peak current increased, however for 3600 s the peak current drastically diminished to a value even lower than that obtained for 1200 s.

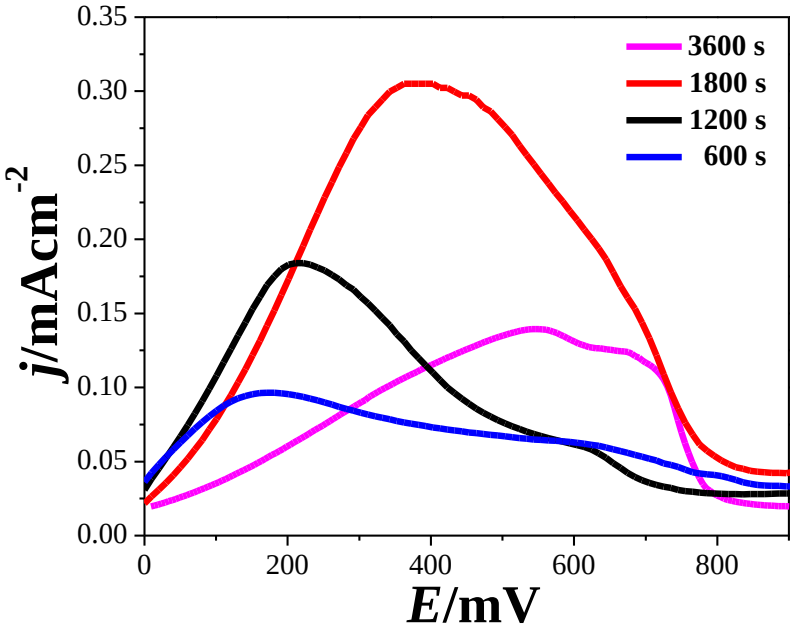

Figure 7. Comparison of linear voltammograms recorded in the system TiO_2-NTBs/Pd in 0.5 M H_2SO_4 containing 1.0 M HCOOH at 50 mVs^{-1} for different Pd electrodeposition times indicated in the figure.

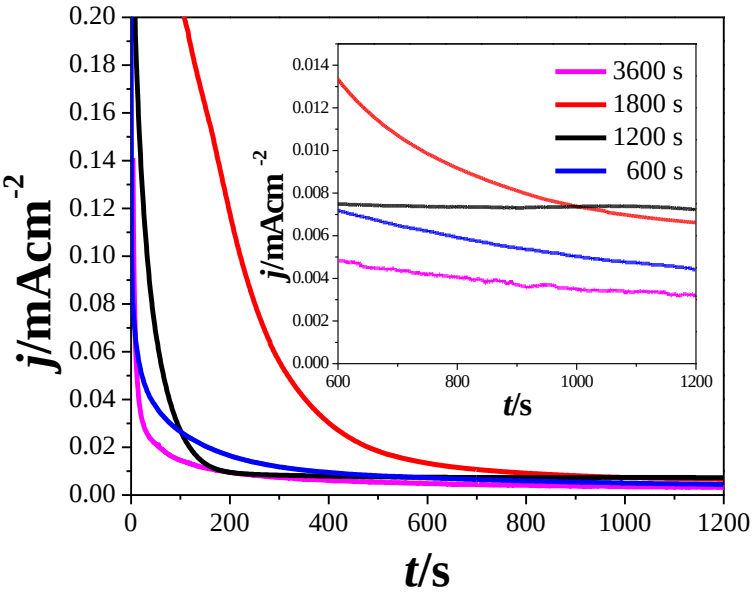

Figure 8. Comparison of potentiostatic current density transients recorded in the system TiO_2-NTBs/Pd in 0.5 M H_2SO_4 containing 1.0 M HCOOH at 250 mV for different Pd electrodeposition times indicated in the figure. The inset shows a close up region of the current for longer times.

Figure 8, shows the experimental current transients obtained during HCOOH oxidation using different TiO_2-NTBs/Pd electrodes after applying a 250 mV constant potential. From this figure, see the inset, it can be noted that the highest steady state current density, j_d, was recorded for the TiO_2-NTBs/Pd electrode obtained after 1200 s Pd deposition time. Straightforward, this TiO_2-NTBs/Pd electrode exhibited the best results for a Pd electrodeposition time of 1200 s; once again the performance at 3600 s was not a commendable electrocatalyst. From these results, it becomes apparent that when Pd is deposited onto the TiO_2-NTBs, there is a catalytic effect toward HCOOH electrochemical oxidation, although in larger quantities, the beneficial effect of the TiO_2-NTBs substrate becomes subdued.

Figure 9 depicts the effect of the number of voltammetric cycles recorded during HCOOH electrochemical oxidation using the TiO_2-NTBs/Pd electrode, formed after 1200 s Pd electrodeposition. It becomes evident that even when the current density maximum tends to decrease slightly with the number of cycles, a significant part of the catalytic activity of this electrode toward HCOOH oxidation remains, which suggests that the Pd surfaces have not been substantially blocked (poisoned) by any reaction products [32] or simply due to catalyst's deactivation [33]. The HCOOH oxidation at Pt surfaces occurs through a dual-path mechanism [34-36], which involves direct oxidation of HCOOH to CO_2 (dehydrogenation) or CO formation and oxidation (dehydration), thus becoming the poisoning intermediate. CO is adsorbed on the active sites of Pt surfaces and completely blocks the activity for the HCOOH oxidation. On the other hand, it has been demonstrated that the HCOOH oxidation on Pd surfaces follows the direct pathway (dehydrogenation) [35-37].

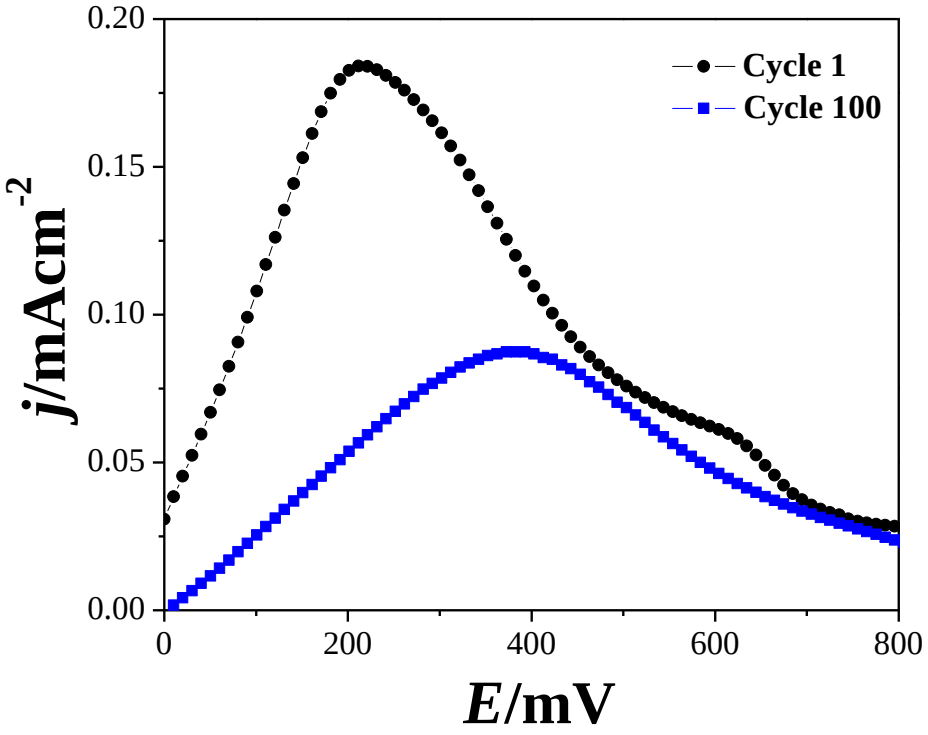

Figure 9. Comparison of linear voltammograms (cycle 1 and 100) recorded in the system TiO_2-NTBs/Pd in 0.5 M H_2SO_4 containing 1.0 M HCOOH at 50 mVs^{-1} for the electrode formed after 1200 s Pd electrodeposition time.

4. CONCLUSIONS

The HCOOH electro-oxidation from an aqueous acid solution, on third generation TiO_2 nanotubes modified with Pd, was evaluated. The response of the modified electrode was found to be the best alternative compared with the bare Ti or with the electrode composed only of TiO_2-NTBs. The best response for the HCOOH oxidation corresponded to the TiO_2-NTBs-Pd electrode, where the Pd was electrodeposited during 1200 s. The results show that this type of electrodes, without further modification can be adequately used for the organic molecules oxidation, such as HCOOH and for its application in power generation devices, i.e. fuel cells.

ACKNOWLEDGEMENTS
JIAG is grateful to Programa para el Desarrollo Profesional Docente en Educación Superior of the UAEM for the postdoctoral research support. JUC, MGMY, MARR, MTRS and MEPP thank the SNI for the distinction of their membership and the stipend received. MGMY, MEPP, MARR and MTRS wish to thank SEP-PRODEP for the financial support through RedNIQAE. We thank the Divisional Centre for Microscopy UAM-A and J. Olvera-García for fruitful discussion regarding this work.

References

1. A. Manthiram, A. Vadivel Murugan, A. Sarkar and T. Muraliganth, *Energy Environ Sci*., 1 (2008) 621.
2. J. Larminie, A. Dicks and M.S. McDonald, Fuel cell systems explained, John Wiley & Sons Ltd, (2003) Chichester, West Sussex, England.
3. W. Vielstich, A. Lamm and H.A. Gasteiger, Handbook of Fuel Cells: Fundamentals, Technology, and Applications, John Wiley & Sons Ltd, (2003) Somerset, NJ, US.
4. N.A.M. Barakat, M.A. Abdelkareem, G. Shin and H.Y. Kim, *Int. J. Hydrogen Energy*, 38 (2013) 7438.
5. C. Rice, S. Ha, R.I. Masel, P. Waszczuk, A. Wieckowski and T. Barnard, *J. Power Sources*, 111 (2002) 83.
6. X. Yu and P.G. Pickup, *J. Power Sources*, 182 (2008) 124.
7. N.M. Aslam, M.S. Masdar, S.K. Kamarudin and W.R.W. Daud, *APCBEE Procedia*, 3 (2012) 33.
8. Y. Xia, T.-T. Nguyen, S. Fontana, A. Desforges, J.-F. Maréché, C. Bonnet and F. Lapicque, *J. Electroanal. Chem*., 724 (2014) 62.
9. D. Dixon, J. Melke, M. Botros, J. Rathore, H. Ehrenberg and C. Roth, *Int. J. Hydrogen Energy*, 38 (2013) 13393.
10. J. Yang, X. Liu and X. Du, *ECS Electrochem Lett.*, 3 (2014) B30.
11. V. Celorrio, D. Plana, J. Flórez-Montaño, M.G. Montes de Oca, A. Moore, M.J. Lázaro, E. Pastor and D.J. Fermín, *J. Phys. Chem. C.*, 117 (2013) 21735.
12. J. Jiang and A. Kucernak, *J. Electroanal. Chem.*, 520 (2002) 64.
13. H. An, H. Cui, D. Zhou, D. Tao, B. Li, J. Zhai and Q. Li, Electrochim. Acta, 92 (2013) 176.
14. W. Ju, R. Valiollahi, R. Ojani, O. Schneider and U. Stimming, *Electrocatalysis*, 7 (2015) 149.
15. S. Bong, S. Uhm, Y.-R. Kim, J. Lee and H. Kim, *Electrocatalysis*, 1 (2010) 139.
16. M. Rezaei, S.H. Tabaian and D.F. Haghshenas, *Electrocatalysis*, 5 (2014) 193.

17. J. Moreira, P. del Angel, A.L. Ocampo, P.J. Sebastián, J.A. Montoya and R.H. Castellanos, *Int. J. Hydrogen Energy*, 29 (2004) 915.
18. S. Woo, J. Lee, S.-K. Park, H. Kim, T.D. Chung and Y. Piao, *J. Power Sources*, 222 (2013) 261.
19. G. Yang, Y. Sun, Z. Yuan, P. Lü, X. Kong, L. Li, G. Chen and T. Lu, *Chinese J. Catal*., 35 (2014) 770.
20. T. Toda, H. Igarashi, H. Uchida and M. Watanabe, *J. Electrochem. Soc.*, 146 (1999) 3750.
21. C.A. Reiser, L. Bregoli, T.W. Patterson, J.S. Yi, J.D. Yang, M.L. Perry and T.D. Jarvi, *Electrochem. Solid-State Lett*., 8 (2005) A273.
22. S. Iijima and T. Ichihashi, *Nature*, 363 (1993) 603.
23. V. Idakiev, Z.Y. Yuan, T. Tabakova and B.L. Su, *Appl. Catal. A*., 281 (2005) 149.
24. L.-S. Zhong, J.-S. Hu, Z.-M. Cui, L.-J. Wan and W.-G. Song, *Chem. Mater*., 19 (2007) 4557.
25. L.A. Estudillo-Wong, A.M. Vargas-Gómez, E.M. Arce-Estrada and A. Manzo-Robledo, *Electrochim. Acta*, 112 (2013) 164.
26. N.R. Elezović, B.M. Babić, V.R. Radmilovic, L.M. Vračar and N.V. Krstajić, *Appl. Catal. B*., 206 (2013) 140.
27. H. Yu, J. Ma, Y. Zhang, X. Zhang, W. Shi, *Electrochim. Acta*, 56 (2011) 6498.
28. M. Wang, D.J. Guo, H.L. Li, *J. Solid State Chem*., 178 (2005) 1996.
29. M. Shao, J.H. Odell, S.-I. Choi and Y. Xia, *Electrochem. Commun*., 31 (2013) 46.
30. V. Celorrio, M.G. Montes de Oca, D. Plana, R. Moliner, D.J. Fermín and M.J. Lázaro, *Int. J. Hydrogen Energy*, 37 (2012) 7152.
31. L.-l. Fang, Q. Tao, M.-f. Li, L.-w. Liao, D. Chen and Y.-x. Chen, *Chin J Chem Phys*., 23 (2010) 543.
32. S. Garbarino and L.D. Burke, *Int. J. Electrochem. Sci*., 5 (2010) 828.
33. S.M. Baik, J. Han, J. Kim and Y. Kwon, *Int. J. Hydrogen Energy*, 36 (2011) 14719.
34. M. Llorca, J. M. Feliu, A. Aldaz, J. Clavilier, *J. Electroanal. Chem*., 376 (1994) 151.
35. M. Arenz, V. Stamenkovic, T. J.Schmidt, K. Wandelt, P. N. Rossa, N. M. Markovic, *Phys. Chem. Chem. Phys*., 5 (2003) 4242.
36. M. Baldauf, D. M. Kolb, *J. Phys Chem*., 100 (1996) 11375.
37. N. Hoshi, K. Kida, M, Nakamura, M. Nakada, K. Osada, *J. Phys Chem. B*., 110 (2006) 12480.